SOX9-positive pituitary stem cells differ according to their position in the gland and maintenance of their progeny depends on context.

135 characters

Running Title: Stem cells and adaptative response in the pituitary.

Karine Rizzoti[a,1], Probir Chakravarty[b], Daniel Sheridan[a], and Robin Lovell-Badge[a,1].

[a] Laboratory of Stem Cell Biology and Developmental Genetics, The Francis Crick Institute, London NW1 1AT, UK

[b] Bioinformatics core, The Francis Crick Institute, London NW1 1AT, UK

[1] authors for correspondence karine.rizzoti@crick.ac.uk and robin.lovell-badge@crick.ac.uk

ABSTRACT

Stem cell (SC) differentiation and maintenance of resultant progeny underlie cell-turnover in many organs, but it is difficult to pinpoint the contribution of either process. In the pituitary, a central regulator of endocrine axes, adult SCs undergo activation following target organ ablation, providing a well-characterized paradigm to study an adaptative response in a multi-organ system. Here we used single cell technologies to characterize SC heterogeneity and mobilization together with lineage tracing. We show that SC differentiation occurs more frequently than thought previously. In adaptative conditions, differentiation increases and is more diverse than demonstrated by the lineage tracing experiments. Detailed examination of SC progeny suggests that maintenance of selected nascent cells underlies SC output, highlighting a trophic role for the microenvironment. Analyses of cell trajectories further predict pathways and potential new regulators. Our model provides a valuable system to study the influence of evolving states on the mechanisms of SC mobilization.

Teaser: Pituitary stem cells are diverse and differentiate more than thought but only selected progeny persist according to need.

INTRODUCTION

The pituitary gland controls the three major endocrine axes, reproduction, stress and metabolism, and is involved in homeostasis; all under control of the hypothalamus. Its function requires modulation of hormonal output over short and long terms, and this is regulated at several levels, including rates and patterns of hormone secretion, synthesis and storage, and changes in endocrine cell numbers. Different mechanisms are known to underlie endocrine cell emergence: division of endocrine cells, differentiation from resident SCs and transdifferentiation, although the relevance of the latter is unclear. Under normal and stable conditions, it is thought that division from endocrine cell types is sufficient for the typical low cell turnover seen in the pituitary (*1*). This has been directly shown in corticotrophs using a genetic trick where cell division induces apoptosis of POMC expressing cells. A gradual loss of corticotrophs is observed in these pituitaries in support of the role of these endocrine cells in their own replacement (*2*). In agreement, long term lineage tracing of adult SOX2 and SOX9 +ve pituitary SCs in steady-state conditions suggests that SCs differentiate rarely and thus do not significantly participate in cell turnover (*3*) (*4*). Furthermore, adult ablation of the SCs does not appear to affect pituitary function (*5*). In contrast, when the regenerative or adaptative potential of the gland is stimulated, either by endocrine cell ablation (*6*) or target organ ablation (*3*) respectively, SC-derived new endocrine cells of the appropriate type emerge. In this latter paradigm, differentiation from SCs appears to be the main process underlying emergence of new corticotrophs after adrenalectomy (Ax) (*2*), providing a well characterized multi-organ system to explore mechanisms of SC activation.

Here, we explore the characteristics of pituitary SC fate acquisition using single cell approaches combined with lineage tracing analyses. We observe that SOX9 +ve pituitary SCs comprise several functionally distinct sub-populations, located in the ventral and dorsal part of the epithelium lining the pituitary cleft and in the anterior pituitary parenchyma. We then explored mechanisms underlying SC mobilization following target organ ablation through characterizing cell trajectories and gene regulatory networks (GRNs) potentially involved in cell fate acquisition. We observed that while fate acquisition of the targeted cell type (corticotrophs after Ax and gonadotrophs after gonadectomy) was efficiently induced, differentiation toward all endocrine cell types unexpectedly also took place. Examination of longer-term outcomes using lineage tracing further showed that only a proportion of the differentiated progeny is retained, specifically that of the targeted cell type. More precisely, we only observe SC-derived corticotrophs after Ax, and lactotrophs in females, following Selective Estrogen Receptor Modulator (SERM) treatment. Therefore, while pituitary SC differentiation appears both more frequent and diverse than previously thought, our results suggest that the selective maintenance of nascent cells, according to perceived pathophysiological need and likely sex-dependent hormonal cues, is an important regulatory step controlling their adaptative response. Our model thus allows characterisation of this response following pathophysiological manipulations that may well relate to normal life-changing events, such as puberty, pregnancy and lactation.

82
83
84 RESULTS
85
86 Distinct regulatory pathways govern AL and IL SC identity
87
88 The anterior lobes of three *Sox9*$^{iresGFP/+}$ adult male pituitaries were dissociated and the
89 transcriptome of single GFP +ve cells analysed after fluorescence activated cell sorting
90 (FACS), as previously described (*3*). After quality checks, 1993 cells were retained for
91 further analysis; clustering was performed by generating UMAP plots. Three major clusters
92 were identified (Fig.1A). Co-expression of *Sox2* and *Sox9* in clusters 0 and 2 (Fig.1B,
93 Sup.Fig.1), representing 69% of the cells, suggested that these were likely to represent SCs.
94 The presence of two SC clusters had previously been reported in whole pituitary datasets (*7*)
95 (*8*). The remaining cluster (1), representing 24% of the dataset, comprised cells where *Sox*9
96 was detected, but where *Sox2* was greatly reduced or absent. Finally, cells each expressing a
97 different hormone and the corresponding lineage specifying factors, were grouped within a
98 single smaller cluster (3) representing 3% of the cells (Fig.1B, Sup.Fig.1). SOX9 is not
99 expressed in any endocrine cell in quiescent conditions (*9*). However, we observed some rare
100 SOX9;ACTH +ve cells, and more numerous GFP;ACTH +ve cells in *Sox9*$^{iresGFP/+}$ animals
101 exclusively after activation of the SCs by pituitary target organ ablation (*3*) (Sup. Fig.2). This
102 suggests that differentiating, and recently differentiated cells are present in the SOX9iresGFP
103 fraction due to persistence of the GFP, which correlates with what has been suggested to
104 happen in both human and mouse pituitaries, where hormone positive cells were included in
105 the SC compartment of whole pituitary single cell RNAseq datasets (*10*). In addition, a small
106 proportion of contaminating pituitary cells (estimated to represent 25% of cluster 3) is likely
107 to be present (Sup.Fig.3). Therefore, most cells present in cluster 3 are likely to represent
108 cells committed toward an endocrine fate, with the largest population (41% of cluster 3 cells)
109 expressing *Prolactin*.
110
111

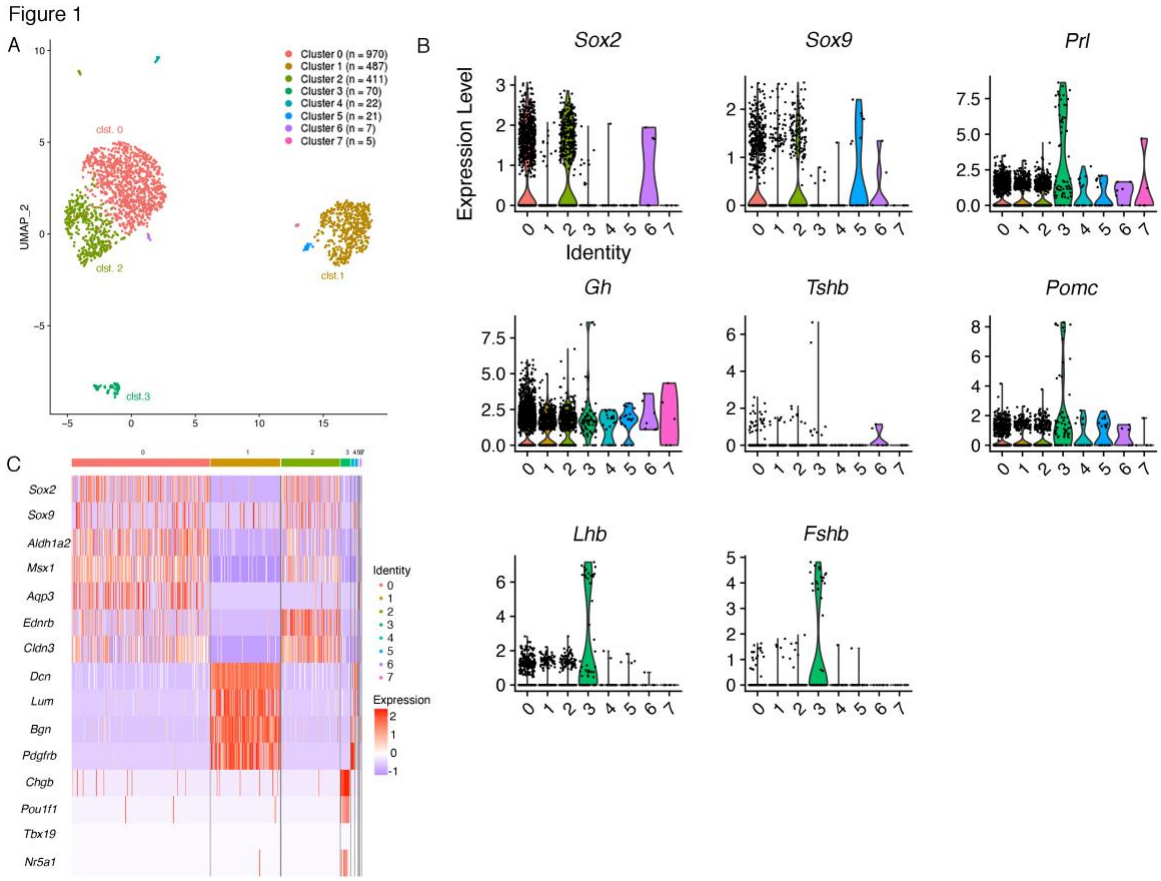

Figure 1: Single cell analysis of the *Sox9*$^{iresGFP/+}$ population in male pituitaries.

A) UMAP clustering of *Sox9*$^{iresGFP/+}$ cells.
B) Expression levels of *Sox2* and *Sox9* were examined to identify SCs (*9*) while genes encoding for hormones (*Gh*, *Prl*, *Tshβ*, *Lhβ*, *Fshβ*, *Pomc*) were examined to distinguish committed cells (*Pou1f1* for somatotrophs, lactotrophs and thyrotrophs.
C) Heatmap displaying selected markers for the main clusters.

The two SC clusters were further explored. Analysis of differentially expressed genes (DEG) (Fig.1C, Sup.Fig.1B) shows that clusters 0 and 2 are relatively similar and are mostly distinguished by differences in levels of expression of specific genes. One notable exception is *Aqp3*, encoding for a water channel, which is specific for cluster 0. In contrast, *Aldh1a2*, encoding for an enzyme involved in retinoic acid (RA) synthesis, and the transcription factor *Msx1* were preferentially present in cluster 0, while *Ednrb*, encoding for the endothelin B receptor, and the cell adhesion molecule *Claudin3* were both expressed at higher levels in cluster 2. RA is required during pituitary morphogenesis (*11*) (*12*) and *Msx1* interacts with SOX2 for *Prop1* regulation (*13*), while nothing is known about *Ednrb* or *Claudin3* in pituitary SCs. Conservation of most of these markers in SCs from whole pituitary datasets (*7*) (*8*) suggests that our two SC clusters correlate with those observed by others. In the gland, expression of the five markers is restricted to SCs (Fig.2, Sup. Fig.4). In the epithelium lining the cleft, cluster 0 markers ALDH1a2 and MSX1 are expressed exclusively on the AL side (Fig.2 A,, Sup.Fig4B), while cluster 2 markers EDNRB and CLAUDIN-3 (Fig.2 C,D) are

present on both sides. In the parenchyma ALDH1a2, MSX1 and CLAUDIN-3 co-localise with SOX2/9 while expression of EDNRB is not detectable. In situ hybridisation for *Ednrb* confirms a clear enrichment in cleft lining cells (Sup.Fig.5). AQP3, whose transcript is present in about half of cluster 0 cells, is exclusively detected in the parenchymal SCs, revealing further heterogeneity between cleft-lining and parenchymal populations. In addition, it is only expressed in a subset of SOX2;SOX9 positive parenchymal SCs (Fig.2B), demonstrating the existence of parenchymal subpopulations. Examination of the five markers in scRNAseq datasets from whole pituitaries (21) confirms that the strongest, and sometimes exclusive, expression is seen in SCs (Sup. Fig.4). All together, these results suggest that cluster 0 is enriched in anterior lobe SCs, while cluster 2 has a more generic pituitary SC identity.

Pathway analysis in cluster 0 (Sup Table.1) highlighted activity of the NOTCH and WNT pathways and presence of Ephrin signalling, as previously reported in pituitary SCs (*14*) (*15*). Cluster 2 cells are characterised by expression of cytoskeleton remodelling and adhesion genes consistent with the EMT-like process required during pituitary progenitor cell fate acquisition (*16*). In conclusion, regionalisation of these two SC subpopulations is underlined by the expression of genes involved in the activity of specific regulatory pathways, such as retinoic acid signalling in AL SCs. Further investigation is required to understand what distinguishes AQP3 positive and negative parenchymal SCs.

Folliculo-stellate (FS) cells are specialised AL glial cells (*17*). These express S100b in the rat, but not in the mouse ((*18, 19*), Sup. Fig.6). To clarify their relationship with SCs, we examined expression of *Aldolase C*, a marker for rodent FS cells (*19*) and of *Slc152a*, which encodes a transporter responsible for the FS specific import of AMCA (*20*). Both are selectively present in SCs, in clusters 0 and 2 (Sup.Fig.6A). Furthermore, in a whole pituitary dataset, *Sox2* and *Aldoc* are exclusively present in the SC cluster (Sup.Fig.6B). All together these results confirm, as suggested earlier (*9, 21*) (*22, 23*), that in the mouse FS and SCs are overlapping populations.

In conclusion, single-cell analysis of the $Sox9^{iresGFP/+}$ pituitary fraction successfully resolved heterogeneity of this population, suggesting differential activity of signalling pathways, and clarified the relationship between SCs and FS cells.

-

Figure 2

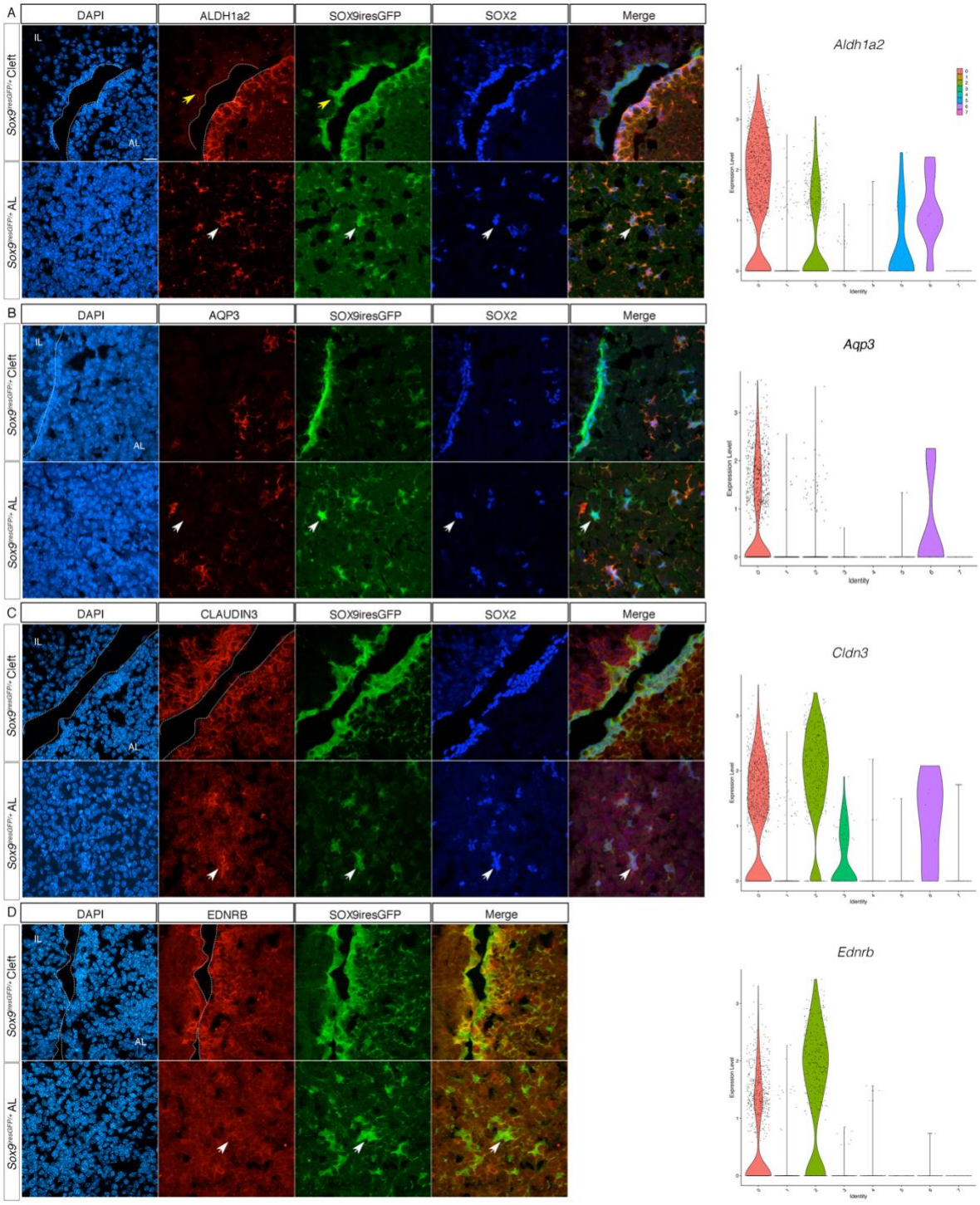

Figure 2: Differential expression of SC cluster markers.

A) Co-immunofluorescence for ALDH1A2, GFP and SOX2 in a male SOX9iresGFP pituitary section. ALDH1A2 is exclusively expressed in SOX2;SOX9 AL SC (yellow arrow shows its absence from IL SC, and white arrow shows its expression in parenchymal SC). *Aldh1a2* violin plot shows enrichment in cluster 0.

B) Co-immunofluorescence for AQP3, GFP and SOX2 in a male SOX9iresGFP pituitary section. AQP3 is expressed in 66% of SOX2 +ve parenchymal SC (white arrow shows SOX2;SOX9iresGFP parenchymal SC not expressing AQP3; counting was performed on n=3 animals). *Aqp3* violin plot shows enrichment in cluster 0.
C) Co-immunofluorescence for CLAUDIN3, GFP and SOX2 in a male SOX9iresGFP pituitary section. CLAUDIN3 is exclusively expressed in SOX2;SOX9 SC. *Cldn3* UMAP shows enrichment in cluster 2.
D) Co-immunofluorescence for EDNRB and GFP in a male SOX9iresGFP pituitary section. EDNRB is exclusively expressed in SOX9 cleft SC. *Ednrb* UMAP shows enrichment in cluster 2. Similar expression profiles were observed in females for all markers.
The scale bar in A represents 10 μm for all panels. White arrows show absence of expression in parenchymal SC. AL, anterior lobe, IL intermediate lobe.

<u>A novel population of parenchymal SOX9;PDGFRβ +ve cells</u>

Cluster 1, representing 25% of the cells, is characterised by expression of PDGFRβ (Fig.1C, Fig.3E). *In situ*, PDGFRβ;SOX9 +ve cells are exclusively detected in the parenchyma. Expression of SOX9 in these double +ve cells is weaker than in SCs (Fig.1B, Fig.3A) and SOX2 is not detected (Fig.1B , Fig.3B). In contrast with the *in silico* analysis, only 8±1.62% SD of parenchymal SOX9 +ve cells express PDGFRβ in males (Fig.3C). This discrepancy could be due either to an over-representation of cluster 1 cells, because epithelial SCs are more difficult to recover than parenchymal cells, or to the difficulty in detecting the cells by immunofluorescence. We observe significantly fewer PDGFRβ;SOX9 +ve cells in females than in males (1.3±0.6% SD, p= 0.029, Fig.3C). PDGFRβ +ve pituitary cells are known to comprise a mural vascular network (*18*). While we did not attempt to fully characterize the SOX9;PDGFRβ population, we observe some SOX9;PDGFRβ cells in close contact with capillaries, displaying a pericyte like morphology (Fig.3D). In the embryo, vascular and mural cells have an extra-Rathke's pouch origin, as they emerge from immigrating neural crest cells (*24, 25*). Because cluster 1 cells do not express the generic pituitary marker *Pitx1* (Fig.3E), we analysed a potential neural crest origin by performing WNT1-Cre lineage tracing. 79 ± 3.1% SEM of SOX9;PDGFRβ cells (n=130 cells from 4 males) derive from WNT1-Cre +ve cells (Fig3C, F) while in females only 47.5 ± 5.5% SEM of the cells derive from the neural crest (n= 57 cells from 3 females, p= 0.024). Therefore, we propose that cluster 1 comprises a sexually dimorphic mural network with a dual embryonic origin. The pituitary capillary network, which controls endocrine output, adapts according to the physiological context and this is particularly important for gonadotroph function (*26*). The sex differences we observe may be related to this aspect.

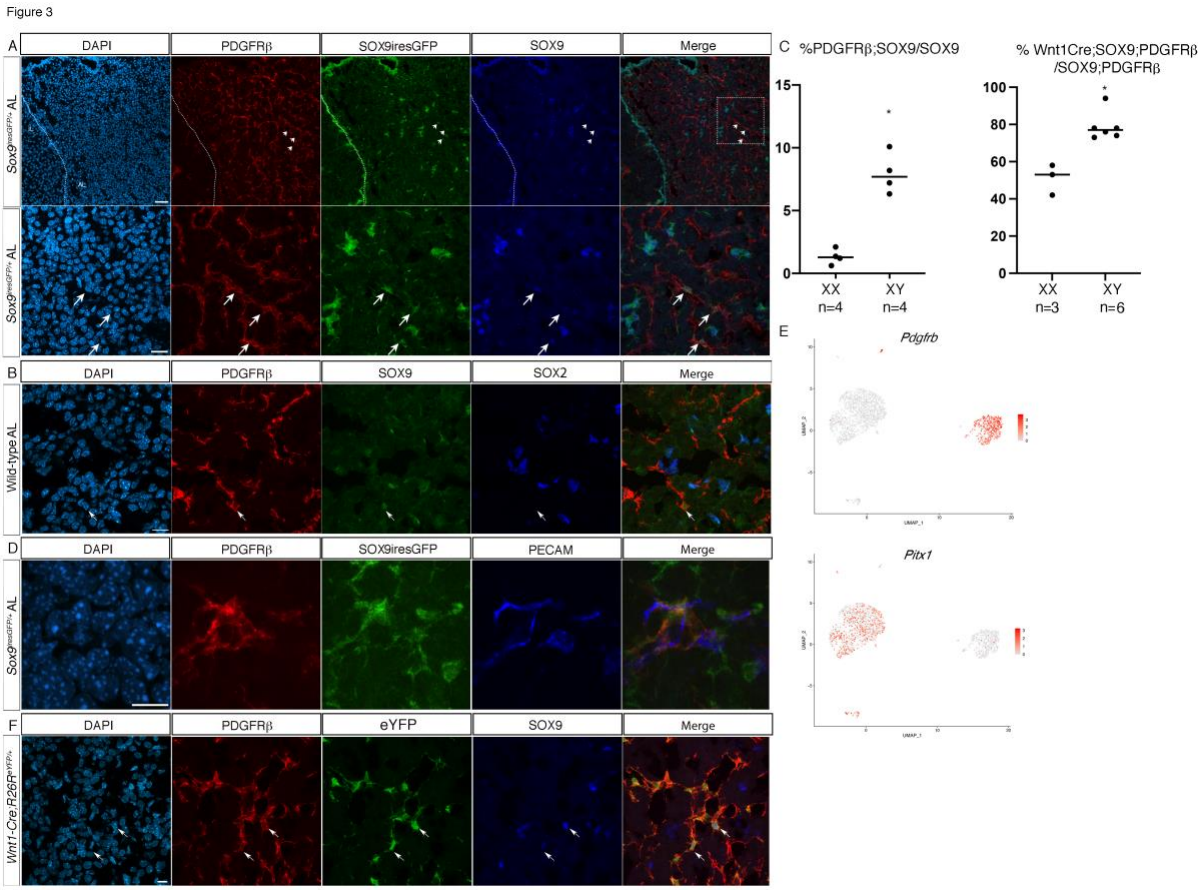

Figure 3: Characterisation of a SOX9;PDGFRβ +ve AL cell population.

A) Co-immunofluorescence for PDGFRβ, GFP and SOX9 in a SOX9iresGFP male AL section. Triple +ve cells are indicated (arrows). The lower panels represent the magnification of the region indicated on the merge panel above. The dotted line indicates the pituitary cleft.

B) Co-immunofluorescence for PDGFRβ, GFP and SOX2 in AL. A SOX9;PDGFRβ +ve cell which is negative for SOX2 (arrow).

C) Percentage of GFP;SOX9;PDGFRβ/GFP;SOX9 +ve cells in *Sox9iresGFP* male and female AL sections (average 500 SOX9 cells counted/animal, p = 0.029). In SOX9iresGFP pituitary sections, parenchymal SOX9; GFP were captured (Sup.Table.4). Amongst these, the percentage of those also positive for PDGFRβ cells was determined. Percentage of SOX9;PDGFRβ +ve cells of neural crest origin (p = 0.024; Mann Whitney test). In Wnt1Cre;R26ReYFP pituitary sections, Sox9;PDGFRb cells were captured. Amongst these, the percentage of those also positive for Wnt1Cre;ReYFP cells was determined (Sup.Table.4).

D) Co-immunofluorescence for PDGFRβ, GFP and PECAM in a Sox9iresGFP AL section showing a SOX9;PDGFRβ +ve cell resembling a pericyte bridging PECAM +ve capillaries.

E) UMAP for *Pitx1* and *Pdgfrβ* showing that *Pdgfrβ* +ve cluster 1 cells do not express *Pitx1*.

F) Co-immunofluorescence for PDGFRβ, eYFP and SOX9 in a *Wnt1-Cre;R26R*^{eYFP} AL section. Triple +ve cells are shown (arrows).

The scale bars represent 50 µm and 20 µm for A (upper and lower panels respectively) and 10 µm for D and F.

234
235 All endocrine cell types are present in the *Sox9*$^{iresGFP/+}$ +ve compartment after SC
236 mobilization.
237
238 We then performed sc-RNAseq on activated SCs. Target organ ablation induces a transient
239 proliferative wave in the gland, mostly affecting SCs, which can then give rise to new
240 endocrine cells (*2, 3, 27*). We analysed the transcriptome of *Sox9*$^{iresGFP/+}$ male cells 4 days
241 after removing the adrenals, the testes or both. We integrated these datasets with that
242 obtained from unchallenged animals and obtained a similar clustering of SCs (Fig.1,
243 Fig.4A,B, Sup. Fig.7A). A pairwise comparison for proportion test limited to SC clusters
244 demonstrates a significant increase in proliferative cells after target organ ablation
245 (Sup.Fig.7B), as previously shown (*3*). We also observe the emergence of distinct hormone
246 +ve clusters representing in total 25 to 30% of all cells (Fig.4A,B) compared to 3.5% in the
247 unchallenged dataset, suggesting increased differentiation. Target organ ablation is associated
248 with increased secretion, and sometimes cell numbers, of the endocrine population regulating
249 the resected organ. However, regardless of the glands removed, all endocrine cell lineages
250 emerge in the Sox9iresGFP +ve fraction. While we expected *Pomc* +ve cells to prominently
251 feature after Ax, these were outnumbered by *Prl* and *LHb*;*FSHb* +ve cells (Sup. Fig. 7C).
252 Similarly, gonadectomies were expected to trigger commitment toward the gonadotroph cell
253 fate, but *Gh* +ve cells were mostly observed. To characterise these *Sox9*$^{iresGFP/+}$;hormone +ve
254 cells we compared them with endocrine cells by integrating our datasets with one from whole
255 pituitaries (*28*). *Sox9*$^{iresGFP/+}$;hormone +ve cells cluster with endocrine cells (Fig.4C, D).
256 Therefore, they represent differentiated cells, at least transcriptionally. In conclusion, target
257 organ ablation induces differentiation of SCs, but there is an unexpected lack of specificity in
258 the endocrine cell types produced, with all hormonal markers being up-regulated.

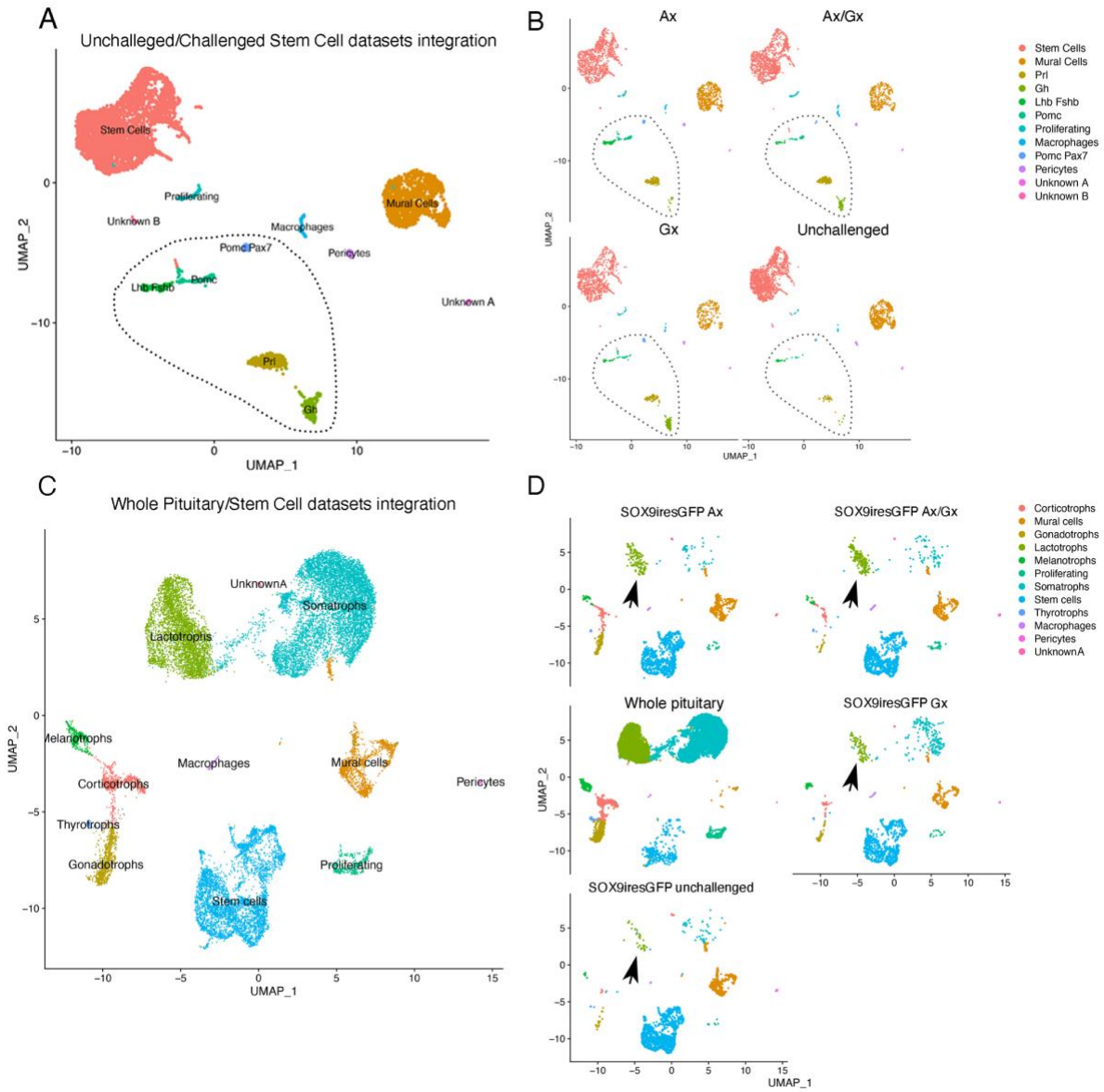

Figure 4: Target organ ablation induces differentiation toward multiple endocrine lineages. A) UMAP clustering for integrated datasets from sorted *Sox9*$^{iresGFP/+}$ cells from unchallenged, adrenalectomized (1915 cells), gonadectomized (1546 cells) and both adrenalectomized and gonadectomized (1880 cells) animals, 4 days after surgery. B) UMAP clustering split by experiment showing the contribution of cells originating from each dataset. Cells expressing all pituitary hormones are present (dotted lines) in all conditions. C) UMAP clustering for integrated datasets from sorted *Sox9*$^{iresGFP/+}$ cells and a whole pituitary dataset (*28*). D) UMAP clustering split by experiment show that hormone +ve cells present in the *Sox9*$^{iresGFP/+}$ cells cluster with endocrine cells (black arrow pointing to lactotrophs).

Analyses of cell trajectories after Ax.

We decided to focus on Ax because it represents the most efficient stimulus of SC differentiation after target organ ablation (*3*). We added a new time point at day 2 after Ax

275 and a sham control. These new datasets were then integrated (Fig.5A) with our initial dataset
276 (Fig.1) and the one performed 4 days after Ax (Fig.4). UMAP clustering indicated that SCs
277 were present in four distinct clusters (Sup. Fig.4). In addition to the *Ednrb* and *Aldh1a2*
278 clusters, two SC clusters (SC3 and SC4) emerged (Fig.5A). These were mostly but not
279 exclusively populated by cells from the new datasets (Sup. Fig.8). While more cells were
280 sequenced in these new datasets (up to 3 times more), we used a different chemistry (see
281 material and methods) which, despite Seurat batch correction tools, may explain detection of
282 more genes and cells resulting in emergence of these clusters. SC3 was characterised by
283 higher expression of markers also present in the *Ednrb* and *Aldh1a2* clusters. SC4, mostly
284 derived from the Ax+48h00 dataset, showed co-expression of SC and endocrine markers
285 suggesting that it represents cells in a transitioning phase (Sup. Fig.9). Finally, endocrine cell
286 clusters were detected (Sup. Fig.9), as observed previously (Fig.4).
287 In sham operated animals, 4.5% of hormone expressing cells, mostly *Prl* +ve, were present,
288 confirming our observations in unchallenged animals (Sup. Table 2). 48 hours after Ax, the
289 proportion of hormone +ve cells had increased to 11%, and this had again doubled after 4
290 days. Because Sox9iresGFP expression stops as cells differentiate the increasing proportion
291 means that commitment toward differentiation augments during the 4 days following
292 ablation. A pairwise proportion test between the 2 new datasets, sorted identically on the
293 same day, showed that a shift occurs from SC4; while the proportion of cells from each
294 dataset in the 3 SC clusters were comparable, from SC4 the proportion of cells from the Ax
295 dataset becomes significantly increased compared to the control, fitting with its transitioning
296 phase profile (Fig.5B, Sup. Fig.9). At this shorter time point, 48 h00 after adrenal ablation,
297 corticotrophs are the most significantly increased cell type, while 4 days after surgery they
298 were outnumbered by lactotrophs. This sharp and transient increase could represent the
299 specific SC response to adrenals ablation.
300 We then performed trajectory analyses after principal component analysis (PCA) using
301 Slingshot (*29*) using exclusively Ax+48h and Sham Ax+48h datasets. Trajectories finishing
302 at each endocrine cell type were discovered, with a common root through SC clusters *Ednrb*,
303 *Aldh1a2,* proliferative cells and SC4, then ending at each endocrine cell type (Fig.5C, Sup.
304 Fig.10 and 11). In the corticotroph trajectory (Fig.5D), the expression pattern of 2245 genes
305 significantly correlates with pseudotime (Fig.5F). The expression of known SC markers
306 (*Ednrb*, *Sox2*, *Sox9*, *Aldh1a2*) and signalling pathway members (*Notch2*, *Hes1*, *Hey1* and
307 *Wnt4*, *Fzd2*, *Sfrp5*) was gradually lost. Pathway analyses further suggest keratin filament
308 remodelling, in agreement with epithelial to mesenchymal transition during differentiation.
309 *Ismn1* (*30*) and *Prop1*(*16*), which are involved in cell fate acquisition, are also present during
310 early phases. Conversely, the corticotroph specifier and marker genes *Neurod1*, *Ascl1*, *Tbx19*,
311 *Pomc* and *Creb3l2* (*31*) are upregulated as cells differentiate. A sharp transition occurs as
312 *Prop1* is upregulated and is characterised by a transient up-regulation of *Pou1f1* lineage and
313 gonadotroph (*Fshb*) genes. Comparisons with trajectories from other lineages reveal similar
314 trajectories with a transient up-regulation of unrelated lineages markers (Sup.Fig.11). This
315 could reflect permissive chromatin remodelling as endocrine cell fate acquisition occurs.

316 SCENIC analyses were then performed to explore GRNs (*32*) and compare them between the
317 different endocrine lineages (Fig.5G, H, Sup.Fig.11). As expected *Sox2* and *9* regulons

318 featured in SC clusters while *Ascl1*, *Neurod1* and *Creb3l2* were present in corticotrophs. The
319 thyroid (*Thra*) and the androgen (*Ar*) hormone receptor regulons featured in corticotroph-
320 differentiating SCs, suggesting that SCs can respond to peripheral signals. New pituitary
321 GNRs were also discovered, such as those involving *Runx1* and *Irf9* whose expression was
322 validated in SCs (Fig.5E, G, H). RUNX1 (RUNt-related transcription tactor 1) is known to
323 control adult skin SC maintenance by regulating WNT signalling (*33*) and is shared between
324 the corticotroph and gonadotroph trajectories. IRFs (Interferon Regulatory Factors) are
325 modulators of cell growth and differentiation beside their anti-viral functions. IRF9
326 associates with phosphorylated STAT1:STAT2 (Signal Transducer and Activator of
327 Transcription) dimers, and all are present in our four endocrine SCENIC analyses (*34*).
328 Finally, several RA factors were also present in all trajectories, supporting RA involvement
329 during endocrine cell differentiation (Fig.5H).

330 In conclusion, by adding new datasets, we validated our previous observations suggesting a
331 low differentiation rate of SCs, mostly into lactotrophs in the intact and sham operated
332 animal. We refined the dynamics of the adaptative response after mobilization, showing a
333 transient peak of corticotroph differentiation 48 hours after Ax. Finally, we were able to infer
334 endocrine cell trajectories revealing common and exclusive factors during each endocrine cell
335 fate acquisition.
336
337

Figure 5

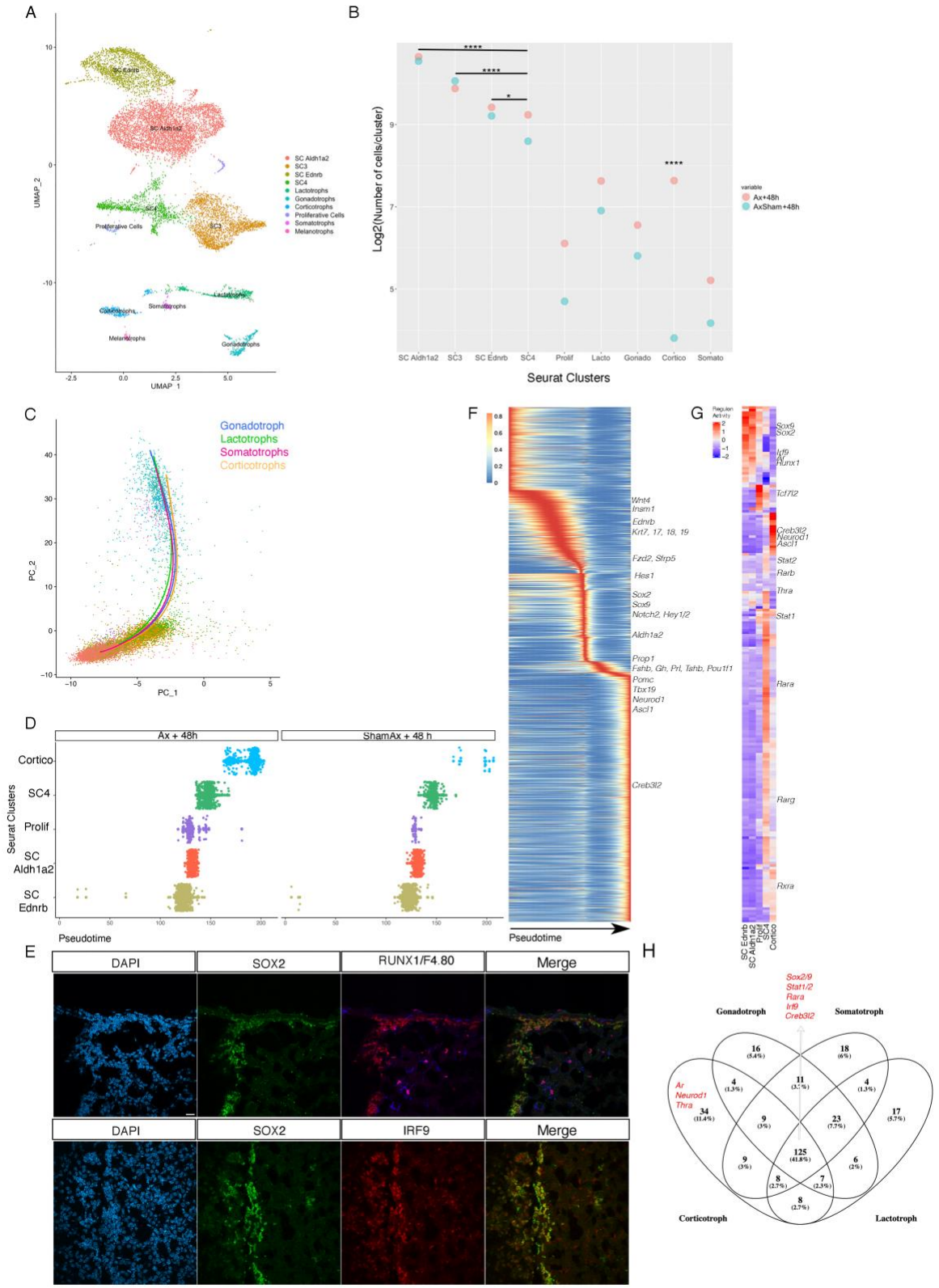

Figure 5: Trajectory analyses following Ax.

A) UMAP clustering for integrated datasets from sorted GFP +ve cells from unchallenged, adrenalectomized and sham + 48 h, and + 4 days, all from *Sox9*$^{iresGFP/+}$ pituitaries. The data has been filtered to remove mural and vascular cells and outliers. Cluster colour scheme is constant throughout the figure. B) Pairwise comparison for proportion test performed on

344 adrenalectomized and sham + 48h. The proportion of corticotrophs after Ax is significantly
345 different from all other cluster distributions. The proportion of cells in cluster SC4 is
346 significantly different from all other SC cluster distributions (Sup. Table2). C) Representation
347 of endocrine cell trajectories on the PCA plot for integrated dataset. D) Proportion of
348 cells/cluster in the corticotroph trajectory comparing Ax and sham Ax. Differentiation is
349 occurring predominantly after Ax. E) Immunofluorescence on pituitary sections validates
350 RUNX1 and IRF9 expression in SOX2 +ve SCs. RUNX1 is also expressed in F4.80 +ve
351 macrophages. F) Heatmap of 2245 genes associated with the corticotroph trajectory. G)
352 Heatmap of SCENIC analysis on the corticotroph trajectory. H) Venn diagram of the
353 common and unique regulons between the different endocrine trajectories (Sup.Fig. 11).
354

355 Selective maintenance of SC progeny

356 To examine predictions from our transcriptomic analyses, we performed two different types
357 of lineage tracing experiment. First, we directly assessed expression of hormonal markers on
358 plated *Sox9*$^{iresGFP/+}$ FACSorted single cells by immunofluorescence in males and females, 4
359 days after Ax or sham-surgery. Second, to follow mobilized SCs further, we used *Sox9*$^{ires-}$
360 $^{CreERT2/+}$; *R26R*$^{EYFP/+}$ animals and examined progeny 10 to 11 days after Cre induction (a
361 week after surgery since induction is mostly performed for 3 days before surgery).

362 All hormone +ve cell types were found in the GFP +ve fraction in both experimental and
363 control *Sox9*$^{iresGFP/+}$ animals, which matches our transcriptomic analyses (Fig.6 A, B).
364 Following Ax, the number of POMC +ve cells increased the most, in agreement with our
365 earliest dataset (Ax+ 48h). However, even if less efficiently stimulated after Ax, the
366 proportion of most other endocrine cell types was comparable to that of corticotrophs. This
367 again reflected our transcriptomic data. More precisely, we also observed a slight increase in
368 somatotroph emergence in both sexes, while lactotrophs and to a reduced extent rare
369 gonadotrophs appear to increase only in females.

370 We then carried out lineage tracing in *Sox9*$^{ires-CreERT2/+}$; *R26R*$^{EYFP/+}$ animals (Fig.6C). We
371 examined the endocrine cell types predicted to be mostly induced by the single cell analysis
372 (Sup.Fig.3C) plus corticotrophs, since we knew these are present in the SC progeny after Ax
373 (*3*) . In contrast with our previous results (Fig.6A), examination of pituitary sections
374 exclusively revealed the presence of POMC;eYFP +ve corticotrophs after Ax, in comparable
375 numbers in both sexes (Fig.6C). In females, we additionally observed lactotrophs, and did so
376 even without performing target organ ablation. Quantification of lactotroph emergence on
377 dissociated pituitaries confirmed the sex bias (Fig.6D). Correcting for CreERT2 induction
378 efficiency, we estimate that in females SCs contribute to 0.6% of the total population of
379 lactotrophs and these SC-derived lactotrophs represent 2% of the eYFP +ve population
380 (Fig.5F).

381 The two genetic tools we used, *Sox9*^{iresGFP} and *Sox9*$^{ires-CreERT2/+}$, display inherent distinctions,
382 such as use of high-dose of the SERM tamoxifen, and purposes, where these may impair
383 direct comparisons. However, while results from both transcriptomic analyses and
384 immunofluorescence demonstrate that endocrine cells of all types are produced in
385 comparable numbers in the short term, we clearly observe that corticotrophs are the only

386 endocrine cells remaining in long-term lineage tracing experiments in males. This indicates a
387 selective maintenance of nascent endocrine cells.

388 Alternatively, hormone positive cells could acquire expression of SOX9 after surgeries,
389 leading to the presence of SOX9;hormone +ve cells in the SOX9iresGFP fraction but not in
390 the SOX9CreERT2 animals because tamoxifen was given before SC mobilization. There is
391 no supporting evidence for this to happen, while we know that SCs differentiate (SOX9+ve
392 cells become hormone +ve). Furthermore, tamoxifen is known to persist in mice so we
393 should still be able to see these cells in our lineage tracing experiments even if SOX9
394 becomes up-regulated after the surgeries (*35*). Finally, this discrepancy in the presence of
395 hormone+ve cells in short-term versus long-term lineage tracing already exists in the intact
396 animal because we see these cells our unchallenged and sham single cell RNAseq
397 experiment; but ours and others' lineage tracing analyses did not reveal any significant
398 differentiation in normal conditions (*3, 4*). Therefore, we think that the most likely
399 explanation is the selective maintenance of a proportion of the SC progeny.

400 To further explore the sex bias in SC-derived lactotrophs, we administered tamoxifen to P0
401 $Sox9^{ires\text{-}CreERT2/+}$; $R26R^{EYFP/+}$ pups and quantified differentiation into lactotrophs once they
402 reached adulthood. There was no significant difference in the proportion of SC-derived
403 lactotrophs between males and females (Fig.5E), as previously observed (*3*). Therefore, male
404 SC-derived lactotrophs can be produced, but this is temporally restricted. Furthermore,
405 because the proportion of lactotrophs generated from male and female pups is similar, this
406 suggests that tamoxifen, which can interfere with estrogen action, induces lactotroph
407 emergence. If lactotroph emergence was a continuous process in females their proportion
408 would have been far superior to that observed in males. Our results thus reveal a temporal
409 window of sensitivity in males, while female SCs remain responsive to the lactotroph
410 promoting effect of tamoxifen until adulthood. It is unclear how E2 signalling is altered, and
411 whether SC differentiation is induced or maintenance of nascent lactotrophs permitted.
412 Sexual dimorphism in SC activity has also been reported in another endocrine organ, the
413 adrenals, where androgens regulate cell-turnover (*36*).
414

Figure 6

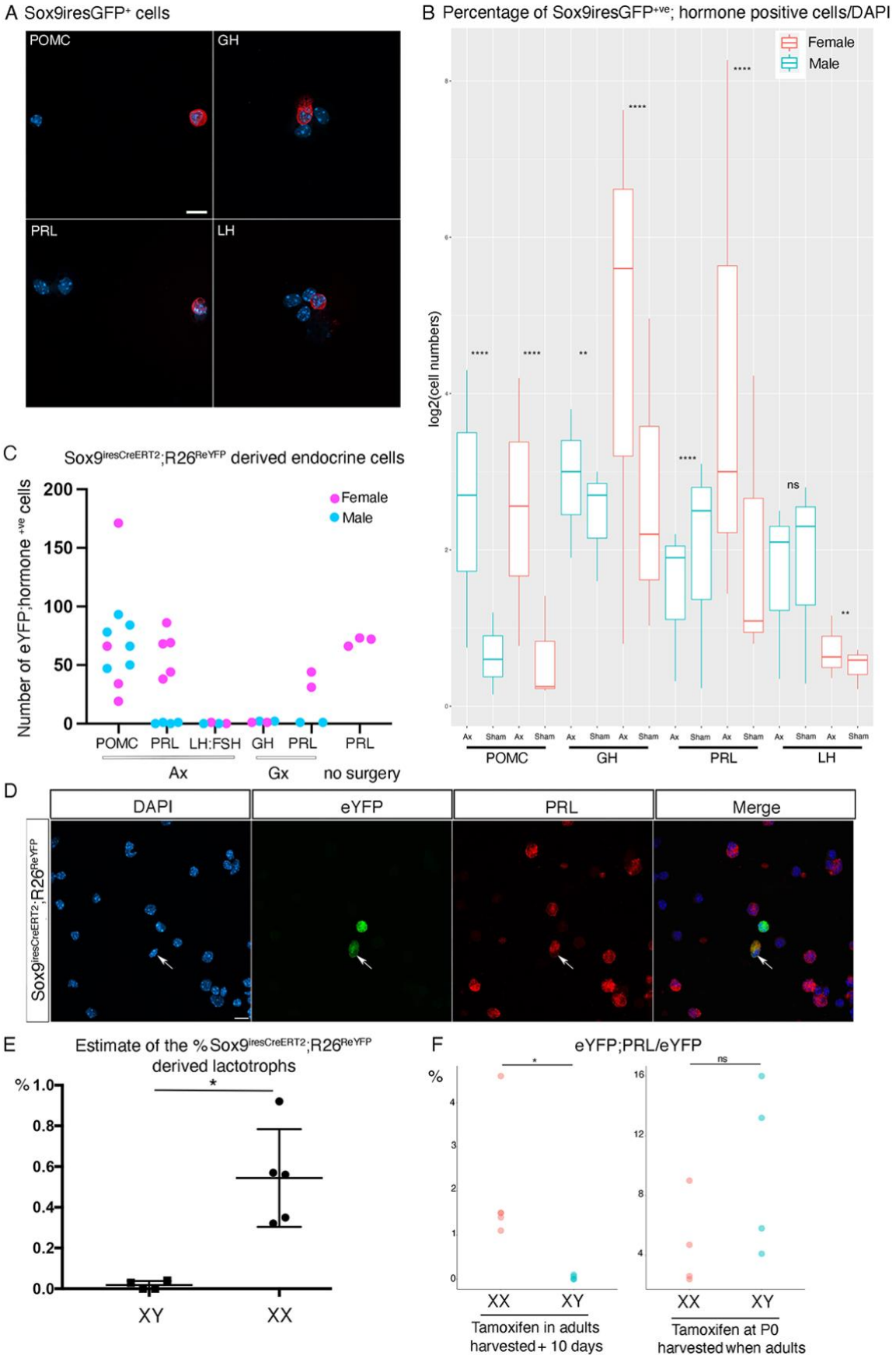
A Sox9iresGFP+ cells
POMC
GH
PRL
LH
B Percentage of Sox9iresGFP+ve; hormone positive cells/DAPI
Female
Male
log2(cell numbers)
POMC
GH
PRL
LH
C
Sox9iresCreERT2;R26ReYFP derived endocrine cells
Number of eYFP;hormone +ve cells
Female
Male
POMC
PRL
LH:FSH
GH
PRL
PRL
Ax
Gx
no surgery
D
DAPI
eYFP
PRL
Merge
Sox9iresCreERT2;R26ReYFP
E
Estimate of the % Sox9iresCreERT2;R26ReYFP derived lactotrophs
%
XY
XX
F
eYFP;PRL/eYFP
%
XX
XY
Tamoxifen in adults harvested + 10 days
Tamoxifen at P0 harvested when adults

415

416 Figure 6: Analyses of scRNAseq predictions by short and long-term lineage tracing.
417 A) Immunofluorescence for hormonal markers on FACsorted Sox9iresGFP +ve cells from a
418 female 4 days after Ax.
419 B) Percentages of FACSorted Sox9iresGFP +ve cells that are hormone +ve /DAPI. Cell
420 counts were performed on plated cells (shown in A). Pituitaries were harvested 4 days after
421 surgeries. Pairwise for proportion tests were performed to assess significance of differences
422 between Ax and Sham (Sup. Table 3).
423 C) Numbers of hormone;eYFP double +ve cells counted in *Sox9*$^{iresCreERT2/+}$*;Rosa26*^{ReYFP}
424 pituitaries a week after surgeries or 10 days after tamoxifen treatment (no surgery). Counts
425 were performed on comparable samples of whole pituitary sections. Corticotrophs are
426 observed in both sexes after Ax, as previously reported. In contrast, significant numbers of
427 lactotrophs are exclusively observed in females. LH;FSH cells have never been observed
428 after gonadectomies (*3*) and were thus not quantified here.
429 D) Immunofluorescence for eYFP and PRL on dissociated non-sorted
430 *Sox9*$^{iresCreERT2/+}$*;Rosa26*^{ReYFP} female pituitary cells. A PRL;eYFP +ve cell is indicated
431 (arrow).
432 E) Estimation of the percentage of lactotrophs differentiated from SCs. eYFP;PRL +ve cells
433 from *Sox9*^{iresCreERT2}*;Rosa26*^{ReYFP} dissociated pituitaries were counted 10 days after tamoxifen
434 treatment. Numbers were corrected for Cre induction efficiency. Induction efficiency was
435 calculated in each animal as the percentage of SOX9;eYFP/SOX9 +ve cells present in the
436 cleft, which was preserved from dissociation. There is very little proliferation in normal
437 conditions in the cleft SCs, and we thus assumed that the number of eYFP;SOX9 positive
438 cells directly reflected induction efficiency. 0.6% of lactotrophs originate from SCs 10 days
439 after tamoxifen induction in females while we barely observed any in males (Mann-Whitney
440 test performed on angular transformation of percentages, p=0.0159).
441 F) Percentage of PRL;eYFP/eYFP +ve cells counted 10 days after tamoxifen treatment in 8
442 to 10 week-old animals, and in 8 week-old animals that were treated with tamoxifen as pups
443 (eYFP;PRL/eYFP in *Sox9*$^{iresCreERT2/+}$*;Rosa26*^{ReYFP}). The proportion of SCs becoming
444 lactotrophs is significantly higher in adult females compared to males (t-test, p=0.03). This
445 sex bias disappears when tamoxifen is administered in pups (t-test test, p=0.1825). Scale bars
446 represent 10 microns.
447
448 HGF trophic effect on pituispheres suggests that SCs and corticotrophs interact.
449
450 The selective maintenance of specific nascent SC progeny, while the rest are lost, suggests
451 that survival is dependent on local cues in their microenvironment. In the context of Ax, the
452 corticotrophs are a likely source of signals. We thus re-examined our transcriptomic datasets,
453 screening for signalling pathways potentially activated in SCs by corticotrophs. We found
454 that the receptor tyrosine kinase *Met* is selectively upregulated in SCs while its ligand *Hgf* is
455 present both in corticotrophs and pericytes (Fig.7A-C, Sup.Fig 12 (*37*)), suggesting
456 interactions between these cell types. Furthermore, following Ax, the number of SCs
457 expressing *Met* is increased, exclusively in those proliferating (Fig.7D). This suggests a
458 potential trophic effect of HGF on SCs that we explored in pituisphere assays (Fig.7E, F).
459 Upon HGF treatment, the number of pituispheres is on average doubled compared to the

control, demonstrating a trophic effect on SCs. Because the number of corticotrophs is increased after Ax and levels of HGF may thus potentially increase too, this pathway may mediate or at least participate in the increased SC proliferation observed after Ax. In agreement with a trophic role of the pathway in the pituitary, the receptor and its ligand are both widely expressed in human pituitary adenomas (*38*).

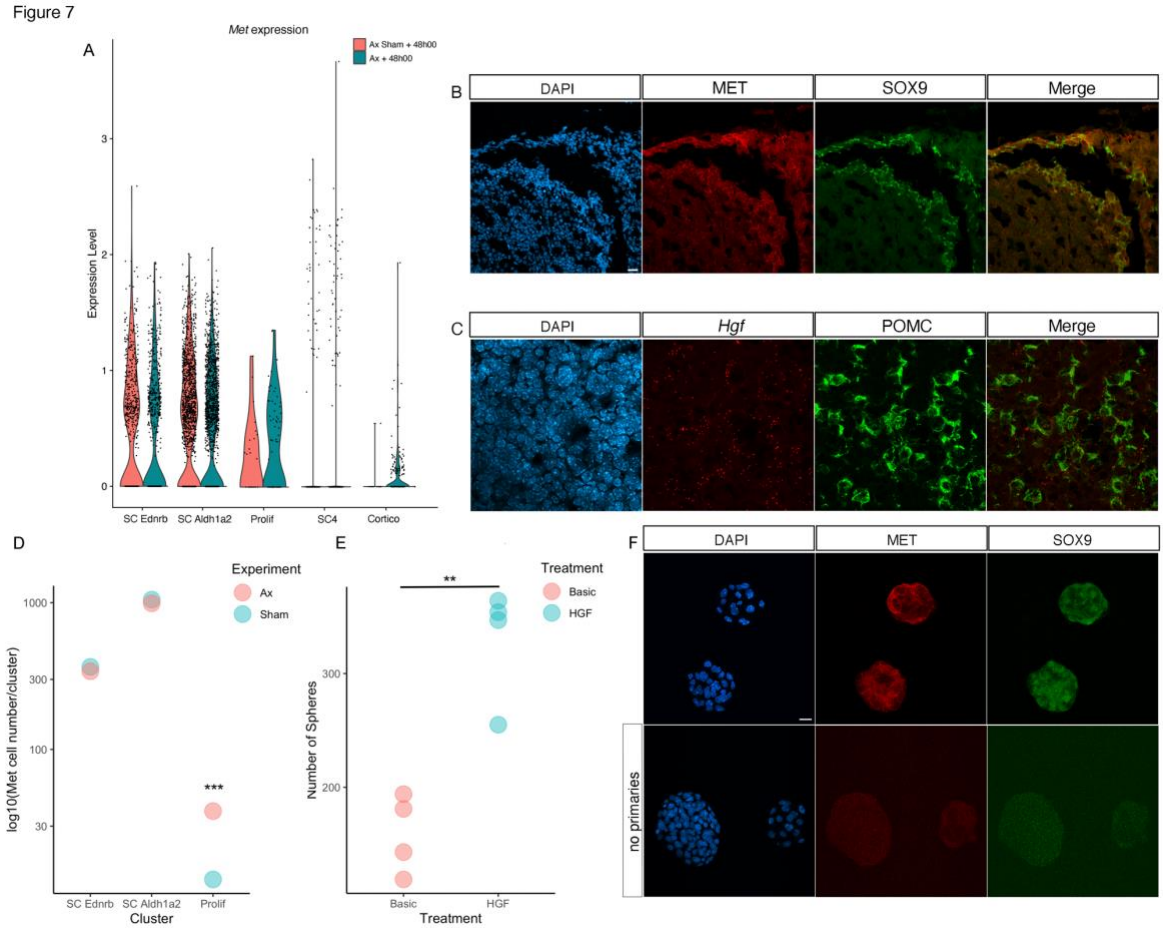

Figure 7: *Met*/MET and *Hgf* are expressed in SCs and corticotrophs respectively and the ligand has a trophic effect on pituispheres.

A) Expression levels of *Met* are shown in clusters belonging to the corticotroph trajectory (Fig.5D). B) Immunofluorescence for MET and SOX9 showing the receptor is expressed in SCs. C) In situ hybridisation (RNAscope) and immunofluorescence for *Hgf* and POMC respectively showing that MET ligand is expressed in corticotrophs. *Hgf* is also predicted to be expressed in pericytes which could explain signal outside corticotrophs. D) More cells express *Met* after Ax specifically in the cluster comprising proliferating cells (Chi-squared test, p= 0.0005, Sup.Table 3). E) More pituispheres form when 100ng/ml HGF is added to basic medium (t-test, p= 0.002, Sup. Table 3, n=4). F) MET is expressed in SOX9 +ve pituispheres. Scale bar represents 20 microns in B and D, and 10 microns in C.

DISCUSSION

While adult pituitary SCs appear superfluous for cell-turnover in the unchallenged animal, their differentiation potential can be stimulated, for example when the function of certain endocrine axes is compromised, such as when adrenals or gonads are ablated (*3*) (*2, 5*). Here we have characterized SC heterogeneity and the modalities of endocrine cell emergence, by examining Sox9iresGFP single cells. We observe that a small percentage of pituitary SCs differentiate in the unchallenged animal, which correlates with single-cell RNAseq analyses performed on both human and mouse pituitaries where the presence of differentiating cells was also detected in the SC compartment (*10*). This proportion increases when SCs are mobilized. The paradigm we applied for SC mobilization, target organ ablation, is known to trigger a specific response in the pituitary: adrenal ablation results in increased ACTH while gonadectomy is associated with increased gonadotropins. However, although there was a significant induction of corticotroph cell fate acquisition shortly after ablation, we unexpectedly observed increased differentiation toward all AL endocrine cell types. Nevertheless, in the longer term, lineage tracing experiments show that it is exclusively the targeted endocrine cell type that is maintained in the SC progeny. Therefore, following differentiation, selective maintenance of specific nascent cells is likely to be an important process regulating pituitary SC endocrine cell output, and it seems likely that this is controlled by the SC microenvironment. Increased sensitivity of nascent pituitary cells to apoptosis had been suggested before (*27*), and shown to increase after target organ ablation, in agreement with our results. Selective fitness of surviving cells in the embryo relies on access to particular trophic factors (*39*). In our Ax paradigm, the pituitary targets of the ablation, the corticotrophs, represent a likely source of signals, a notion re-enforced by the trophic effect of HGF we observe on pituispheres. Similarly, estrogen is known to promote lactotroph proliferation and their emergence in embryos (*40*). We previously examined the effects of estrogen on adult pituitary SC differentiation, but the prior administration of tamoxifen in our lineage tracing system may explain why we did not obtain meaningful results((*3*). Here, our data suggest that tamoxifen treatment induces emergence of lactotrophs, both in male and female neonates, but exclusively in adult females. This in turn implies that this process is sensitive to E2, and that male development suppresses it. The presence of lactotrophs in the male SOX9iresGFP fraction, but not after lineage tracing, suggests that their maintenance is promoted in females. However,to further investigate these aspects a tamoxifen independent lineage tracing tool is required. In parallel with the likely role of corticotrophs on SCs after Ax, lactotrophs may be involved in the selective maintenance of nascent PRL cells emerging after tamoxifen treatment, because they are sensitive to its effect, given that prolactin secretion is increased by the SERM (*41*). In addition to the reliance on trophic factors, it is likely that nascent cell maintenance involves integration into homotypic endocrine networks (*42*). This is reminiscent of what is known for nascent neurons that are often produced in excess and whose persistence relies on synaptic connections (*43*). Although focusing on SCs enabled us to uncover novel regulators and unexpected modalities of the adaptative response, our analyses point toward an important role for the microenvironment, and, in our multi-organ system, peripheric factors which are predicted to modulate the SC response. The thyroid (*Thra*) and the androgen (*Ar*) hormone receptors appear active in differentiating SCs, suggesting that they can respond to peripheral signals, and may integrate

this information to regulate pituitary plasticity, as recently proposed (*44*). Further investigations of both local and peripheral interactions are now required to better understand how this adaptative response is regulated in detail.

Differential clustering of SOX9iresGFP +ve SCs, trajectory analyses and *in situ* validation of new markers revealed the activity of region-specific regulatory pathways. In agreement with what had been shown by others (*7*) (*8*), we found two main populations. We show here that these correlate with differential localisation, anterior lobe (ALDH1a2, MSX1 positive) versus more generic AL/IL SC (CLDN3 positive) identity. This suggests that AL and IL SCs are regulated differently. We speculate that RA may be involved in AL SC differentiation, as shown in the embryo (*11*). The downregulation of ALDH1a2 expression in IL SCs which do not differentiate (*2, 45*) provides an additional support to this hypothesis. The enrichment of EDNRb in the cells lining the cleft reveals a further level of heterogeneity between cleft lining and parenchymal cells. In the trajectory analyses, the upstream expression pattern of *Ednrb* implies that the SCs lining the cleft are in a more immature state than those in the parenchyma, which fits with this epithelium constituting the primary pituitary SC niche. Among the 3 endothelin ligands, *Edn3* is the most abundantly expressed in the gland, more precisely in SCs and pericytes (*37*). This suggests that this pathway could function in an autocrine or paracrine way in cleft SCs, because these are not in close contact with capillaries (*42*), which would make an interaction with the latter unlikely. EDNRB signalling has been shown to regulate melanocyte SC regeneration (*46*) and we are currently investigating whether this role is conserved in pituitary SCs. We have furthermore found that a subpopulation of parenchymal SCs is defined by AQP3 expression. It is unclear whether this correlates with the existence of functionally different subpopulations, such as supporting FS cells versus SCs for example, or whether this reflects distinct SC states, but we are now able to identify these cells, and investigate their role. Finally, the presence of RUNX, IFR and STAT regulons during cell differentiation is also of potential interest because of the roles of these factors in different SC contexts, and because they have been shown to interact (RUNX/STAT and IFR/STAT). STAT transcription factors are activated by different cytokines and growth factors, in particular IL6 whose role in the regenerative response of pituitary SCs was recently uncovered (*7*).

Our differentiation trajectories suggest the presence of a common root for all endocrine cell types, which only segregate as the terminal differentiation markers are upregulated in the nascent cells. This process is likely to be fast since cells still contain GFP expressed from *Sox9iresGFP*. ~~It is now important to determine whether the same genes in this common root are associated with the different lineages and when specificity first appears~~. It is tempting to draw a parallel with embryonic pituitary progenitors, because these were similarly shown to all commit at the same stages (*47*). Interestingly, it was proposed that intrinsic factors and cell communication within the developing pituitary underlie specific endocrine cell fate acquisition, which, in a different context and with different modalities and outcomes, is what we hypothesize is happening in our model.

In conclusion, evaluation of single cell transcriptomic predictions with short and long-term lineage tracing experiments has proved a robust strategy revealing novel aspects of pituitary SC adaptative responses. In circumstances where an exceptional pathophysiological need is

perceived, nascent cells of the appropriate type are maintained. Understanding how the new cells can survive will help us to understand how SC input is controlled in the pituitary, but this could also be relevant in other tissues where SC activity appears largely superfluous. Finally, it is notoriously difficult to obtain mature cell types *in vitro* for use in regenerative medicine. Therefore, identifying trophic factors for nascent cells, which may be all that can be obtained for transplantation, appears necessary.

Acknowledgements:

We are grateful for the support from present and past members of the Lovell-Badge lab. We are indebted to the Francis Crick Institute platforms for their excellent support and expertise. We especially thank Jacek Mor from the Biological Research facility for taking excellent care of the animals, Donald Bell from the Advanced Light microscopy, Deborah Schneider-Luftman from Bioinformatics and Biostatistics and experts from the Advanced Sequencing and Histology platforms. We also thank Frederique Ruf-Zamojski and Zidong Zhang from the Icahn School of Medicine at Mount Sinai (New York) for sharing their expertise.
This work was supported by the Medical Research Council, U.K. (U117512772, U117562207 and U117570590) and the Francis Crick Institute which receives its core funding from Cancer Research UK (FC001107), the UK Medical Research Council (FC001107), and the Wellcome Trust (FC001107).

SUPPLEMENTARY FIGURE LEGENDS:

Sup. Figure 1: Expression of known and novel markers in SOX9iresGFP unchallenged dataset.

A) *Sox2* and *Sox9* were used to identify SCs while genes encoding for hormones (*Gh*, *Prl*, *Tshβ*, *Lhβ*, *Fshβ*, *Pomc*) and lineage specific transcription factors were examined to distinguish committed cells (*Pou1f1* for somatotrophs, lactotrophs and thyrotrophs, *Tbx19* and *Pax7* for corticotrophs and melanotrophs, and *Nr5a1* for gonadotrophs). B) Heatmap for the top10cluster markers.

Sup. Figure 2: Co-localisation between SOX9 and ACTH after Ax.

Co-immunofluorescence for GFP, SOX9 and ACTH on sections of pituitaries harvested one week after Ax. Expression of Sox9iresGFP (A) and SOX9 (B) is observed in rare ACTH +ve cells (arrows) exclusively after Ax. The scale bar represents 10 μm for A and 5μm for B.

Sup. Figure 3: Gating strategy for SOX9iresGFP cells.

613 Gating for SOX9iresGFP cells was validated using wild-type animals. The SOX9iresGFP
614 fraction we selected typically represented 1 to 2% of all cells while 0.02% of all cells were
615 falsely sorted in negative controls. This contamination of likely hormonal cells represents a
616 small proportion of the hormonal cells we detect in our unchallenged Sox9iresGFP fraction
617 (3% of 1.9% representing 0.08% of the whole population).
618
619 Sup. Figure 4: Expression of novel SC cell markers in whole pituitary and SC datasets.
620
621 A) UMAP of re-analysed whole pituitary dataset (*28*). This dataset was used to examine
622 levels of expression of *Ednrb* (B), *Aldah1a2* (C), *Cldn3* (D) and *Msx*1(E) to show exclusive
623 or enriched expression in SCs. F) Co-immunofluorescence for MSX1, GFP and SOX9 in a
624 male SOX9iresGFP pituitary section. MSX1 is exclusively expressed in SOX2;SOX9 AL SC
625 (yellow arrow shows its absence from IL SC, and white arrow shows its expression in
626 parenchymal SC). *Msx1* violin plot shows enrichment in cluster 0 of the single cell dataset
627 presented in Fig.1. The scale bar in A represents 10 μm.
628
629
630 Sup. Figure 5: In situ hybridisation for *Ednrb*.
631
632 In situ hybridisation analysis (RNAscope) of *Ednrb* expression confirming higher levels of
633 expression in cleft versus parenchymal SC where low levels of signal can be detected, while
634 levels of *Sox9* expression appear similar in both compartments. The scale bar represents 200
635 μm.
636
637
638 Sup. Figure 6: Expression of FS cells markers in SC and whole pituitary datasets.
639
640 A-C) UMAP for *S100b* (A), *Aldolase C* (B) and *Slc15a2* (C) in our Sox9iresGFP single cell
641 dataset.
642 D-F) UMAP for *S100b* (D), *Sox2* (E) and *Aldolase C* (F) in a whole pituitary dataset (*28*).
643
644
645 Sup. Figure 7: Unchallenged/Challenged integrated analysis.
646
647 A) UMAP clustering and marker analysis for integrated datasets from sorted *Sox9*$^{iresGFP/+}$
648 cells from unchallenged, adrenalectomized, gonadectomized and both adrenalectomized and
649 gonadectomized animals, 4 days after surgery.
650 B) Pairwise comparison for proportion test ('pairwise_prop_test' function [stats R package])
651 on stem cell clusters (circled on UMAP in A). The number of cells assigned to cluster 10
652 corresponding to proliferative cells (see *Top2a* expression in A) is significantly higher in
653 activated stem cells (Sup. Table2).
654 C) Numbers and proportion of specific hormone +ve cells/all hormone +ve cells in each
655 dataset. While we would expect the number of hormone +ve cells to increase after target

organ ablation, as seen here, the fact that we select fewer GFP weak cells in unchallenged animals prevents us from comparing the proportion of hormone +ve cells in unchallenged and mobilized datasets and thus make this conclusion.

Sup. Figure 8: UMAP clustering for filtered integrated analysis split by dataset.

A) UMAP clustering for integrated datasets from sorted SOX9iresGFP +ve cells from unchallenged, adrenalectomized and sham + 48 h, adrenalectomized + 4 days split by dataset. SC clusters 3 and 4 mostly originate from datasets collected 48 hours after surgery.

Sup. Figure 9: Analyses of marker expression on UMAP clustering in Ax integrated datasets.

Markers of SC and hormone-secreting cell types are shown on the UMAP clustering for integrated datasets from GFP +ve cells sorted from *Sox9*$^{iresGFP/+}$ pituitaries from mice that were unchallenged, adrenalectomized and sham + 48 h, adrenalectomized + 4 days.

Sup. Figure 10: PCA clustering for filtered integrated analysis split by dataset.

SC4 cluster cells located in an intermediate position between SC and endocrine cells originate mostly from Ax+48h, which is consistent with mobilization and increased commitment toward differentiation.

Sup.Fig.11: Analysis of endocrine trajectories and regulons.

Heatmaps of genes associated with trajectories and SCENIC analyses for lactotroph, somatotroph and gonadotroph lineages. Representative genes are shown. Known regulators and those in common with the corticotroph analyses (Fig.5 F-H) are displayed on the heatmaps.

Sup. Figure 12: Expression of *Met* and *Hgf* in the whole pituitary dataset.

Expression of *Hgf* was plotted along with *Pomc* and *Pdgfrb* suggesting expression in *Pomc* positive corticotrophs and *Pdgfrb* positive pericytes, while *Met* expression is restricted to *Sox2* positive SCs (from re-analysed dataset (*28*)). The same pattern is observed in a different dataset (*37*).

Sup. Table1: Pathway analysis for clusters 0 and 2.

Gene markers for WT Cluster 0 were used to determine enriched pathways with Metacore using a hypergeometric test. Pathways with an adjusted p value < 0.05 are shown in the table. Genes present in our dataset are highlighted in the top5 pathways.

Sup. Table2: Endocrine cell cluster numbers from Ax integrated dataset (Fig.5)

700
701 Sup. Table 3: Pairwise for proportion test results.
702
703 Sup. Table 4: Counting numbers for Fig. 2, 3, 5 and 6.
704
705 Sup. Table 5: Cell type signatures.
706
707

708 MATERIALS AND METHODS
709
710
711 **Mice**
712
713 All animal experiments carried out were approved under the UK Animals (Scientific
714 Procedures) Act 1986 and under the project licences n. 80/2405 and PP8826065.
715 *Sox9*$^{iresGFP/+}$ (*Sox9*^{tm1Haak}) (*48*), *Sox9*$^{iresCreERT2/+}$ (*Sox9*$^{tm1(cre/ERT2)Haak}$) (*48*), *Wnt1Cre* (*(no*
716 *gene)*$^{tg(Wnt1\text{-}GAL4)11Rth}$) (*49*) and Rosa26$^{ReYFP/ReYFP}$ (*Gt(ROSA)26Sortm1(EYFP)Cos*) (*50*) mice
717 were maintained on a C57Bl6 background.
718 For CreERT2 induction in *Sox9*$^{iresCreERT2/+}$;Rosa26$^{ReYFP/+}$ animals, tamoxifen was
719 administered for 3 consecutive days at a concentration of 0.2mg/g body weight. For
720 *Sox9*$^{iresCreERT2/+}$;Rosa26$^{ReYFP/+}$ pups induction, a single subcutaneous injection of tamoxifen
721 (0.25mg/g body weight) was performed. Target organ ablations were performed as previously
722 described (*3*).
723
724 **Pituitary SC selection**
725
726 The anterior lobe of freshly dissected 8 to 12 week-old pituitaries was minced and incubated
727 for 15mn at 37ºC in 1mg/ml Papain (Sigma 10108014001), 10µg/ml DNAse I (Sigma
728 10104159001) and 10µg/ml Rock inhibitor (Abmole Bioscience M1817) in HBSS (Sigma
729 H9394). pH was adjusted by addition of NaOH. The enzymatic solution was removed, and
730 the cells were mechanically resuspended in HBSS supplemented with DNAse I and Rock
731 inhibitor, as above. Cells were FACsorted for GFP using a large nozzle (100µm) and low
732 pressure (20psi) for optimal cell survival. For immunofluorescence, sorted cells were plated
733 on Superfrost slides for 90 min in a cell culture incubator, fixed 20 min on ice in 4% PFA and
734 immediately processed.
735
736 **Pituisphere culture.**
737
738 Dissociated anterior lobes (see above) of male and female 7 to 12 week-old mice were seeded
739 at 50.10^3 cells/ml in pituisphere medium containing EGF and FGF (*9*). 100ng/ml of HGF
740 (2207-HG-025/CF, R&D systems) was added to this basic medium in treated cultures.
741 Medium was replaced every other day and spheres manually and blindly counted after 7 days.
742 4 independent repeats were performed.
743
744
745 **Single cell sequencing**
746
747 The concentration and viability of the single cell suspension was measured using Trypan
748 Blue and the Eve automatic cell counter (unchallenged and target organ ablation d4 samples)
749 or acridine orange and propidium iodide with the Luna-FX7 automatic cell counter (Ax and
750 Sham control d2 samples). Up to 10,000 cells were loaded on Chromium Chip and

751 partitioned in nanolitre scale droplets using the Chromium Controller and Chromium 10x 3
752 prime v2.0, Chromium Single Cell 3' Reagent Kits User Guide (v2 Chemistry) (unchallenged
753 and target organ ablation d4 samples) or Next GEM Single Cell reagents (3 prime v3.1) (Ax
754 and Sham control d2 samples). Within each droplet the cells were lysed, and the RNA was
755 reverse transcribed. All of the resulting cDNA within a droplet shared the same cell barcode.
756 Illumina compatible libraries were generated from the cDNA using Chromium Next GEM
757 Single Cell library reagents in accordance with the manufacturer instructions (10x
758 Genomics). Final libraries are quality checked using the Agilent TapeStation and sequenced
759 using the Illumina HiSeq4000 or HiSeq2500, read configuration 26-8-0-98 (unchallenged and
760 target organ ablation d4 samples) or NovaSeq 6000, read configuration 28-10-10-90.
761 Where expression of specific genes in the whole pituitary gland is referenced as ((*37*), we
762 used this published dataset on the Loupe browser to examine expression of relevant markers.
763
764 **Bioinformatic analyses**
765
766 Alignment, Seurat analysis, integration and cluster annotation were performed using
767 CellRanger and Seurat. Raw reads were initially processed by the Cell Ranger v.3.0.2
768 pipeline (*51*), which deconvolved reads to their cell of origin using the UMI tags, aligned
769 these to the mm10 transcriptome (to which we added the eGFP sequence
770 https://www.addgene.org/browse/sequence/305137/ to detect eGFP expressing cells) using
771 STAR (v.2.5.1b) (*52*) and reported cell-specific gene expression count estimates. All
772 subsequent analyses were performed in R v.3.6.0 (*53*) using the Seurat (v3) package
773 (*54*). Genes were considered to be 'expressed' if the estimated (log10) count was at least 0.1.
774 Primary filtering was then performed by removing from consideration cells expressing fewer
775 than 50 genes and cells for which mitochondrial genes made up greater than 3 standard
776 deviations from the mean of mitochondrial expressed genes. PCA decomposition was
777 performed and, after consideration of the eigenvalue 'elbow-plots', the first 20 components
778 were used to construct the UMAP plots per sample. Multiple samples, generated in this study
779 and published (*28*), were integrated using 2000 variable genes and Seurat's CCA method.
780 Cluster specific gene markers were identified using a Wilcoxon rank sum test and the top 20
781 genes ranked by logFC per cluster were used to generate a heatmap. Clusters were annotated
782 using label tranfer methods within Seurat using the GSE120410 dataset (*28*). Clusters were
783 further annotated using cell specific signatures (Sup. Table 5).
784 Cell trajectories were identified using the package 'Slingshot' (version 1.4.0) (*29*), using the
785 undifferentiated cluster as a starting point and the PCA co-ordinates. Lineages were identified
786 showing specific trajectories ending in specific differentiated cells. Differential expression of
787 genes between samples were further investigated for the corticotroph lineage with a
788 correlation metric against pseudotime, using the 'gam' package (version 1.20) (*55*). Heatmaps
789 were made using the smoothed expression of differential genes, and the cells are ranked by
790 increasing pseudotime.
791 In order to investigate transcription factor activity along pseudotime, the package SCENIC
792 (*32*) was used. A list of 948 putative mouse regulatory binding sites found in
793 promoter regions of expressed genes were used to identify shared regulatory networks.
794 Regulon activity score per transcription factor was calculated using the AUCell function,

where the enrichment of target genes was measured using the area under the curve of the target gene relative to the expression-based ranking of all genes. The top 200 regulons ranked by activity score were using to generate a binarized heatmap, where the cells were ranked by pseudotime.

Immunofluorescence and RNAscope.

Pituitaries were fixed after dissection by immersion in 4% PFA at 4ºC. Immunofluorescent stainings were performed on cryosections as described (*56*). The following primary antibodies were used: Goat anti-SOX2 (Biotechne, AF2018), rabbit anti-SOX9 (a gift from F. Poulat, IGH Montpellier, France), rat anti-GFP (Nacalai Tesque 04404-84), chick anti-GFP (Invitrogen, A10262), rabbit anti-EDNRb (Abcam 117529), goat anti-MSX1 (R&D system AF5045), rabbit anti-ALDH1A2 (Abcam 75674, after antigen retrieval), rabbit anti-Claudin3 (Abcam ab15102), rat anti-PECAM (BD Pharmigen, 550274), rat anti-PDGFRβ (eBiosciences 14-1402-81), rabbit anti-AQP3 (Alomone Labs, AQP-003, after antigen retrieval) rabbit anti-Runx1 (Sigma, HPA004176), rabbit anti-IRF9 (Cell Signalling, D9I5H), goat anti-Met (R&D, AF 527) and hormone antibodies anti-LH, GH, ACTH and PRL from the National Hormone Peptide Program (A.F. Parlow, Torrance, USA). Slides were then incubated with Alexa Fluor secondary antibodies. Imaging of stained tissue sections was performed on a Leica SPE microscope while imaging of plated cells was done on an Olympus spinning disk microscope.
RNAscope was performed on cryosections following the manufacturer's instructions using *Hgf* (#456511) and *Ednrb* (#473801) probes.

Cell counts

Counts were performed blindly. For dissociated cell counts, slides stained by immunofluorescence were scanned; automated counts were then performed using QuPath (https://qupath.github.io/). For *Sox9*$^{iresCreERT2/+}$;Rosa26$^{ReYFP/+}$;hormone counting on sections, double +ve cells were manually identified and each imaged on a slide representing 1/5 of a pituitary. Images were then reviewed, and double +ve cells counted. All counting results and tests are presented (Sup. Table 3 and 4).

Statistics

Comparisons of the percentages of Sox9;PDGFRβ (Fig.3) were performed after angular transformation using Mann-Whitney test on Prism. Pairwise for proportion test (Sup. Fig4B, Fig.5B, Fig.6B and Sup. Table 3), t-test (Fig.6E , Fig.7D) and Chi squared test (Fig.7) were performed using the Stats R package.

Author contributions:

Conceptualization: KR, RLB
Methodology: KR
Bioinformatic analyses: PC
Investigation: KR, DS
Visualization: KR
Supervision: KR, RLB
Writing—original draft: KR
Writing—review & editing: KR, RLB

Competing interests:

Authors declare that they have no competing interests.

Data and materials availability:

All data are available in the main text or the supplementary materials.
Codes are available on request. Datasets have been submitted (Awaiting confirmation of data deposited at GEO).

BIBLIOGRAPHY

1. A. Levy, Physiological implications of pituitary trophic activity. *J Endocrinol* **174**, 147-155 (2002).
2. D. Langlais, C. Couture, M. Kmita, J. Drouin, Adult pituitary cell maintenance: lineage-specific contribution of self-duplication. *Mol Endocrinol* **27**, 1103-1112 (2013).
3. K. Rizzoti, H. Akiyama, R. Lovell-Badge, Mobilized adult pituitary stem cells contribute to endocrine regeneration in response to physiological demand. *Cell Stem Cell* **13**, 419-432 (2013).
4. C. L. Andoniadou *et al.*, Sox2(+) stem/progenitor cells in the adult mouse pituitary support organ homeostasis and have tumor-inducing potential. *Cell Stem Cell* **13**, 433-445 (2013).
5. H. Roose *et al.*, Major depletion of SOX2(+) stem cells in the adult pituitary is not restored which does not affect hormonal cell homeostasis and remodelling. *Sci Rep* **7**, 16940 (2017).
6. Q. Fu *et al.*, The adult pituitary shows stem/progenitor cell activation in response to injury and is capable of regeneration. *Endocrinology* **153**, 3224-3235 (2012).
7. A. Vennekens *et al.*, Interleukin-6 is an activator of pituitary stem cells upon local damage, a competence quenched in the aging gland. *Proc Natl Acad Sci U S A* **118**, (2021).
8. F. Ruf-Zamojski *et al.*, Single nucleus multi-omics regulatory landscape of the murine pituitary. *Nature communications* **12**, 2677 (2021).

882 9. T. Fauquier, K. Rizzoti, M. Dattani, R. Lovell-Badge, I. C. Robinson, SOX2-expressing
883 progenitor cells generate all of the major cell types in the adult mouse pituitary
884 gland. *Proc Natl Acad Sci U S A* **105**, 2907-2912 (2008).
885 10. Z. Zhang *et al.*, Single nucleus transcriptome and chromatin accessibility of
886 postmortem human pituitaries reveal diverse stem cell regulatory mechanisms. *Cell*
887 *reports* **38**, 110467 (2022).
888 11. L. Y. M. Cheung, S. A. Camper, PROP1-Dependent Retinoic Acid Signaling Regulates
889 Developmental Pituitary Morphogenesis and Hormone Expression. *Endocrinology*
890 **161**, (2020).
891 12. S. Yoshida *et al.*, Retinoic acid signalling is a candidate regulator of the expression of
892 pituitary-specific transcription factor Prop1 in the developing rodent pituitary. *J*
893 *Neuroendocrinol* **30**, e12570 (2018).
894 13. N. Nishimura *et al.*, Search for regulatory factors of the pituitary-specific
895 transcription factor PROP1 gene. *J Reprod Dev* **62**, 93-102 (2016).
896 14. E. Laporte, A. Vennekens, H. Vankelecom, Pituitary Remodeling Throughout Life: Are
897 Resident Stem Cells Involved? *Frontiers in endocrinology* **11**, 604519 (2020).
898 15. S. Yoshida *et al.*, Cell type-specific localization of Ephs pairing with ephrin-B2 in the
899 rat postnatal pituitary gland. *Cell Tissue Res* **370**, 99-112 (2017).
900 16. M. I. Perez Millan, M. L. Brinkmeier, A. H. Mortensen, S. A. Camper, PROP1 triggers
901 epithelial-mesenchymal transition-like process in pituitary stem cells. *Elife* **5**, (2016).
902 17. P. R. Le Tissier, P. Mollard, Renewing an old interest: Pituitary folliculostellate cells. *J*
903 *Neuroendocrinol*, e13053 (2021).
904 18. L. O'Hara, H. C. Christian, N. Jeffery, P. Le Tissier, L. B. Smith, Characterisation of a
905 mural cell network in the murine pituitary gland. *J Neuroendocrinol* **32**, e12903
906 (2020).
907 19. K. Fujiwara *et al.*, Aldolase C is a novel molecular marker for folliculo-stellate cells in
908 rodent pituitary. *Cell Tissue Res* **381**, 273-284 (2020).
909 20. W. Allaerts, H. Vankelecom, History and perspectives of pituitary folliculo-stellate
910 cell research. *Eur J Endocrinol* **153**, 1-12 (2005).
911 21. E. Laporte *et al.*, Decoding the activated stem cell phenotype of the neonatally
912 maturing pituitary. *Elife* **11**, (2022).
913 22. P. A. Fletcher *et al.*, The astroglial and stem cell functions of adult rat folliculostellate
914 cells. *Glia* **71**, 205-228 (2023).
915 23. S. Zhang *et al.*, Single-cell transcriptomics identifies divergent developmental lineage
916 trajectories during human pituitary development. *Nature communications* **11**, 5275
917 (2020).
918 24. S. W. Davis *et al.*, beta-catenin is required in the neural crest and mesencephalon for
919 pituitary gland organogenesis. *BMC Dev Biol* **16**, 16 (2016).
920 25. H. C. Etchevers, C. Vincent, N. M. Le Douarin, G. F. Couly, The cephalic neural crest
921 provides pericytes and smooth muscle cells to all blood vessels of the face and
922 forebrain. *Development* **128**, 1059-1068 (2001).
923 26. P. Le Tissier *et al.*, An updated view of hypothalamic-vascular-pituitary unit function
924 and plasticity. *Nat Rev Endocrinol* **13**, 257-267 (2017).
925 27. L. A. Nolan, A. Levy, A population of non-luteinising hormone/non-
926 adrenocorticotrophic hormone-positive cells in the male rat anterior pituitary
927 responds mitotically to both gonadectomy and adrenalectomy. *J Neuroendocrinol*
928 **18**, 655-661 (2006).

929 28. L. Y. M. Cheung *et al.*, Single-Cell RNA Sequencing Reveals Novel Markers of Male
930 Pituitary Stem Cells and Hormone-Producing Cell Types. *Endocrinology* **159**, 3910-
931 3924 (2018).
932 29. K. Street *et al.*, Slingshot: cell lineage and pseudotime inference for single-cell
933 transcriptomics. *BMC Genomics* **19**, 477 (2018).
934 30. J. E. Welcker *et al.*, Insm1 controls development of pituitary endocrine cells and
935 requires a SNAG domain for function and for recruitment of histone-modifying
936 factors. *Development* **140**, 4947-4958 (2013).
937 31. J. Drouin, The corticotroph cells from early development to tumorigenesis. *J*
938 *Neuroendocrinol* **34**, e13147 (2022).
939 32. S. Aibar *et al.*, SCENIC: single-cell regulatory network inference and clustering. *Nat*
940 *Methods* **14**, 1083-1086 (2017).
941 33. K. M. Osorio, K. C. Lilja, T. Tumbar, Runx1 modulates adult hair follicle stem cell
942 emergence and maintenance from distinct embryonic skin compartments. *J Cell Biol*
943 **193**, 235-250 (2011).
944 34. C. M. Horvath, G. R. Stark, I. M. Kerr, J. E. Darnell, Jr., Interactions between STAT and
945 non-STAT proteins in the interferon-stimulated gene factor 3 transcription complex.
946 *Mol Cell Biol* **16**, 6957-6964 (1996).
947 35. M. Valny, P. Honsa, D. Kirdajova, Z. Kamenik, M. Anderova, Tamoxifen in the Mouse
948 Brain: Implications for Fate-Mapping Studies Using the Tamoxifen-Inducible Cre-loxP
949 System. *Frontiers in cellular neuroscience* **10**, 243 (2016).
950 36. A. Grabek *et al.*, The Adult Adrenal Cortex Undergoes Rapid Tissue Renewal in a Sex-
951 Specific Manner. *Cell Stem Cell* **25**, 290-296 e292 (2019).
952 37. A. Mayran *et al.*, Pioneer and nonpioneer factor cooperation drives lineage specific
953 chromatin opening. *Nature communications* **10**, 3807 (2019).
954 38. X. Z. Hou *et al.*, Expression of hepatocyte growth factor and its receptor c-Met in
955 human pituitary adenomas. *Neuro Oncol* **12**, 799-803 (2010).
956 39. Y. Wang *et al.*, A cell fitness selection model for neuronal survival during
957 development. *Nature communications* **10**, 4137 (2019).
958 40. K. Ogasawara *et al.*, Hormonal regulation of prolactin cell development in the fetal
959 pituitary gland of the mouse. *Endocrinology* **150**, 1061-1068 (2009).
960 41. D. Gonzalez *et al.*, Luteinizing hormone secretion elicited in a ligand-independent
961 activation of progesterone receptor manner at pituitary level in the rat: differential
962 effect of two selective estrogen receptor modulators. *Neurosci Lett* **289**, 111-114
963 (2000).
964 42. P. Mollard, D. J. Hodson, C. Lafont, K. Rizzoti, J. Drouin, A tridimensional view of
965 pituitary development and function. *Trends Endocrinol Metab* **23**, 261-269 (2012).
966 43. W. Kelsch, C. W. Lin, C. P. Mosley, C. Lois, A critical period for activity-dependent
967 synaptic development during olfactory bulb adult neurogenesis. *J Neurosci* **29**,
968 11852-11858 (2009).
969 44. P. R. Le Tissier, J. F. Murray, P. Mollard, A New Perspective on Regulation of Pituitary
970 Plasticity: The Network of SOX2-Positive Cells May Coordinate Responses to
971 Challenge. *Endocrinology* **163**, (2022).
972 45. V. Moncho-Amor *et al.*, SOX2 is required independently in both stem and
973 differentiated cells for pituitary tumorigenesis in p27-null mice. *Proc Natl Acad Sci U*
974 *S A* **118**, (2021).

975 46. M. Takeo *et al.*, EdnrB Governs Regenerative Response of Melanocyte Stem Cells by
976 Crosstalk with Wnt Signaling. *Cell reports* **15**, 1291-1302 (2016).
977 47. S. W. Davis, A. H. Mortensen, S. A. Camper, Birthdating studies reshape models for
978 pituitary gland cell specification. *Developmental biology* **352**, 215-227 (2011).
979 48. K. Furuyama *et al.*, Continuous cell supply from a Sox9-expressing progenitor zone in
980 adult liver, exocrine pancreas and intestine. *Nat Genet* **43**, 34-41 (2010).
981 49. P. S. Danielian, D. Muccino, D. H. Rowitch, S. K. Michael, A. P. McMahon,
982 Modification of gene activity in mouse embryos in utero by a tamoxifen-inducible
983 form of Cre recombinase. *Curr Biol* **8**, 1323-1326 (1998).
984 50. S. Srinivas *et al.*, Cre reporter strains produced by targeted insertion of EYFP and
985 ECFP into the ROSA26 locus. *BMC Dev Biol* **1**, 4 (2001).
986 51. G. X. Zheng *et al.*, Massively parallel digital transcriptional profiling of single cells.
987 *Nature communications* **8**, 14049 (2017).
988 52. A. Dobin *et al.*, STAR: ultrafast universal RNA-seq aligner. *Bioinformatics* **29**, 15-21
989 (2013).
990 53. R. C. Team, R: A language and environment for statistical computing. *R Foundation*
991 *for Statistical Computing, Vienna, Austria.* , (2019).
992 54. T. Stuart *et al.*, Comprehensive Integration of Single-Cell Data. *Cell* **177**, 1888-1902
993 e1821 (2019).
994 55. T. Hastie, gam: Generalized Additive Models. . *R package version 1.20*, (2020).
995 56. K. Rizzoti *et al.*, SOX3 is required during the formation of the hypothalamo-pituitary
996 axis. *Nat Genet* **36**, 247-255 (2004).
997
998